Structures 65 (2024) 106758

Contents lists available at ScienceDirect

Structures

journal homepage: www.elsevier.com/locate/structures

Post-buckling behaviour of corrugated-edge shells: Numerical insights

Matteo Lai [a], Nicola Luigi Rizzi [b], Victor A. Eremeyev [c], Emanuele Reccia [c,*], Antonio Cazzani [c]

[a] Università degli Studi di Cagliari, Direzione Investimenti Manutenzioni e Sostenibilità, DIMS, via Università 40, Cagliari, Italy
[b] Università di Roma Tre, Dipartimento di Architettura, via della Madonna di Monti 40, Roma, Italy
[c] Università degli Studi di Cagliari, Dipartimento di Ingegneria Civile Ambientale ed Architettura, DICAAR, via Marengo 2, Cagliari, Italy

ARTICLE INFO

Keywords:
Nonlinear shells
Corrugated shells
Edge-corrugated shells
Buckling
Instability
Spherical shells
Nervi's Flaminio dome

ABSTRACT

We provided the detailed buckling and post-buckling analysis of corrugated shallow spherical shells. Such shells are extensively used in civil and mechanical engineering. Here the main attention is paid to a corrugation as a key parameter affecting the instability. Three types of corrugation are introduced and discussed. The latter includes the following types: edge corrugated, half corrugated, and fully corrugated shells. Since the effect on instability is highly affected by the imperfections, a customised set of defects is proposed compared to a perfect structure. Several boundary conditions and load cases are analysed. An increase in the load multiplication factors highlights the effects of corrugation in shallow shells mechanics. Being inspired by the fascinating Nervi's Flaminio dome in Rome, we introduce a novel way to improve the shells design against the instability effects.

1. Introduction

Stability of shells constitutes a rather old and developed branch of mechanics of structures, which found a lot of applications in modern engineering, see e.g. [1–4]. On the other hand, unlike buckling of beams and plates, curved structures such as arches and shells demonstrate much more complex behaviour related to high nonlinearity, sensitivity to imperfections, and multiplicity of solutions. For example, if minor geometric deviations from a perfect structure are considered, the non-linear behaviour significantly differs from the ideal one and exhibits a noticeable decrease of the critical load. This essential influence of imperfections was studied by Koiter [5–7]. In the following we restrict ourselves to spherical shells. Considering buckling of a complete spherical shell under uniform pressure one should mention original papers [8,9], where the classical linear eigenvalue analysis under axisymmertic deformations was provided. More general case was studied in [10], where it was proven that one of the solutions is always symmetrical about a diameter, whereas the others show a sinusoidal variation about the diameter. The membrane solution becomes unstable at the critical pressure given by the formula:

$$P_c = 2E\left(\frac{t}{R}\right)^2 \frac{1}{\sqrt{3-3\nu^2}}, \tag{1}$$

where E and ν are Young's modulus and Poisson's ratio, respectively, t the shell thickness and R the radius of the sphere. After the structure has reached P_c, an equilibrium is still possible but the pressure decreases significantly. The buckling mode was found to be a zonal spherical surface harmonic.

Further analysis of spherical shells was given by Hutchinson [11], where the Donnel-Mushtari-Vlasov (DMV) shallow shell theory was used, see also Koiter's lessons [7]. Note, in buckling and post-buckling analysis DMV theory is one of the most used. Nevertheless, the small strain moderate rotations theory [5,12,13] and the exact theory should be also mentioned. A review and a comparison between them are given by Hutchinson [14]. Koiter [15] has provided results about the axisymmetric buckling under uniform pressure of a shallow portion of a spherical shell, clamped along a circular boundary. The solution proposed by Budiansky [13] for the equilibrium of differential equations depends only on the geometrical parameter λ, defined as follows:

$$\lambda = \left[12(1-\nu^2)\right]^{1/4}\sqrt{\frac{R}{h}}. \tag{2}$$

Following the definition by Reissner [16] a shell could be considered a shallow one when "…difference between meridian slope and sloping angle may be disregarded …"; according to that, shallowness requires coarsely that the ratio between the rise of the shell h, and the half-span a, to be less than 1/6. A complete collection of all the major experiments on spherical shells is reported in [17], where a comparison with theoretical results were given. In [17] one can found a significant discrepancy between the theoretical predictions and the experiments. The reasons for such discrepancy can be summarised as follows:

* Corresponding author.
E-mail address: emanuele.reccia@unica.it (E. Reccia).

https://doi.org/10.1016/j.istruc.2024.106758
Received 15 January 2024; Received in revised form 17 May 2024; Accepted 11 June 2024
Available online 18 June 2024

Fig. 1. The Flaminio dome desingned by Nervi (figure courtesy of E. Reccia).

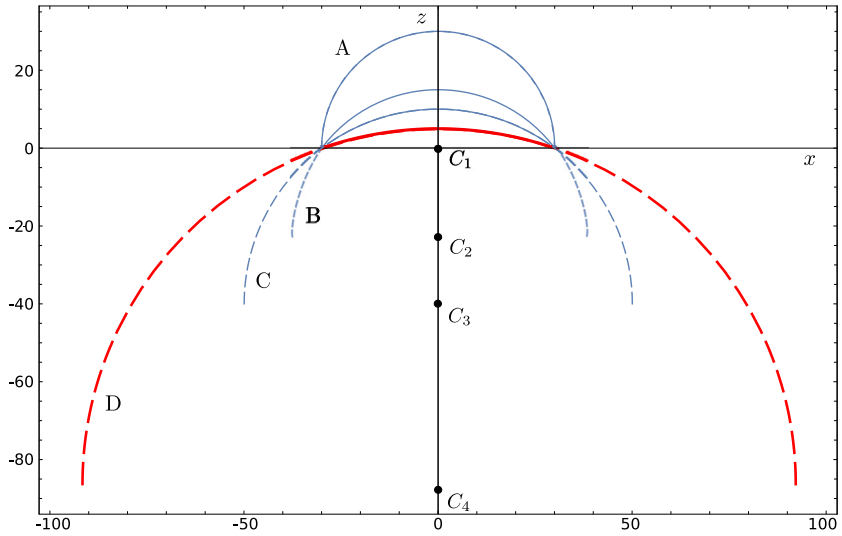

Fig. 2. The representation of four cases for the shallow spherical cross-section, with different rise-to-half-span ratios: A, complete semi-circle with centre C_1 and diameter equal to span; B, C, and D, circles of increasing radios with centres C_2, C_3, C_4, respectively, having the same half-span. The last case D, highlighted in red, is considered here. (For interpretation of the references to colour in this figure legend, the reader is referred to the web version of this article.)

Table 1
Geometric dimension of the spherical cross-section passing through the zx plane.

Case	f	f/l	R	x_0	z_0
	m	–	m	m	m
A	30.00	1.00	30.00	0.00	0.00
B	15.00	0.50	37.50	0.00	−22.50
C	10.00	0.33	50.00	0.00	−40.00
D	5.00	0.17	92.50	0.00	−87.50

1. The behaviour of the shell is highly non-linear, especially in the post-buckling phase. Even in the relatively simple case of circular arches one can see a series of equilibrium paths, see e.g. [18]. The first researchers to point out quantitatively this issue were [19,20]. These authors made it clear that structures deform at significantly lower loads than expected. The reason was attributed to a slight different initial geometry with reference to the theoretical one. This prompted further research into the search for the minimum buckling load. Even more relevant for the purpose of this research was the insight of increasing the flexural stiffness to achieve higher buckling loads. In fact, one way to increase flexural stiffness is to corrugate the shell. The prediction was given by von Kàrmàn [19].
2. The high sensitivity to imperfections and defects, that was clearly the most significant achievement of [21]. Imperfections are defined as deviations from perfect characteristics such as shape, thickness, material properties and load distribution. In practical terms, they are unavoidable and, regardless of the skill, craft and precision of the builders, will always be present in any construction.

Some practical design approaches were suggested in the literature for estimation of a critical load, see e.g. Gioncu [22], Sawires [23], Ramm [24], including analysis of concrete shells by Heyman [25]. It is essential in buckling analysis of reinforced concrete (RC) shells to distinguish between the influence of material and geometrical nonlinearities. It should be pointed out that Ramm suggested to use “buckling phenomena” when the problem involves finite strain and where

Table 2
Eigenvalues and critical loads of a shallow shell (case D) under pressure.

	Hinged edge		Clamped edge	
	Eigenvalue –	Critical load kPa	Eigenvalue –	Critical load kPa
1st	12.723	63.615	12.425	62.125
2nd	12.770	63.850	12.583	62.915
3rd	12.770	63.850	12.583	62.915

Table 3
Eigenvalues of a linear elastic analysis of shallow shells under self-weight.

	Smooth	Edge-corrugated	Half-corrugated	Whole corrugated
1st	16.748	17.259	16.196	25.543
2nd	17.013	17.402	16.196	25.543
3rd	17.013	17.402	16.312	25.553
4th	17.183	17.587	16.312	25.553
5th	17.183	17.587	16.910	27.089
6th	17.329	17.723	16.910	27.089
7th	17.329	17.723	17.639	27.222
8th	17.500	17.869	17.639	27.222
9th	17.500	17.869	18.233	29.095
10th	17.601	17.990	18.233	29.095

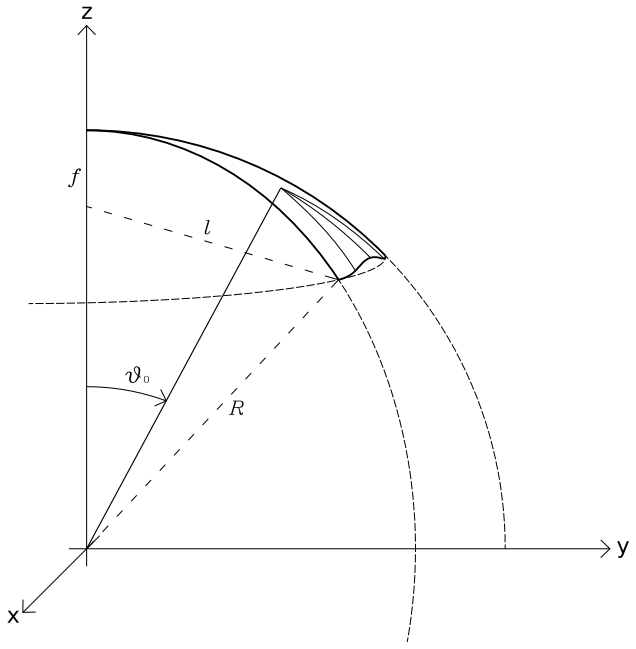

Fig. 3. Spherical coordinate system, with colatitude angles $vartheta_0$.

non linear material effects have little influence on the global behaviour. Last but not least, the ACI recommendations based on IASS recommendations are still valid for design purposes [26].

The aim of this paper is to provide an analysis of corrugated spherical shells including studies of various imperfections similar to whose which one can observe in Nervi's Flaminio dome in Rome, see Fig. 1, and similar corrugated structures. The remainder of the paper is organised as follows. The main content of the paper is presented in Section 2. Here we discussed the relevant geometrical description of a corrugations. A general framework of instability analysis is provided. Then we study the linear stability analysis for different corrugations and loadings. Finally we present post buckling analysis and we provide a discussion of the obtained equilibrium paths. Some final remarks and further applications are given in Conclusions.

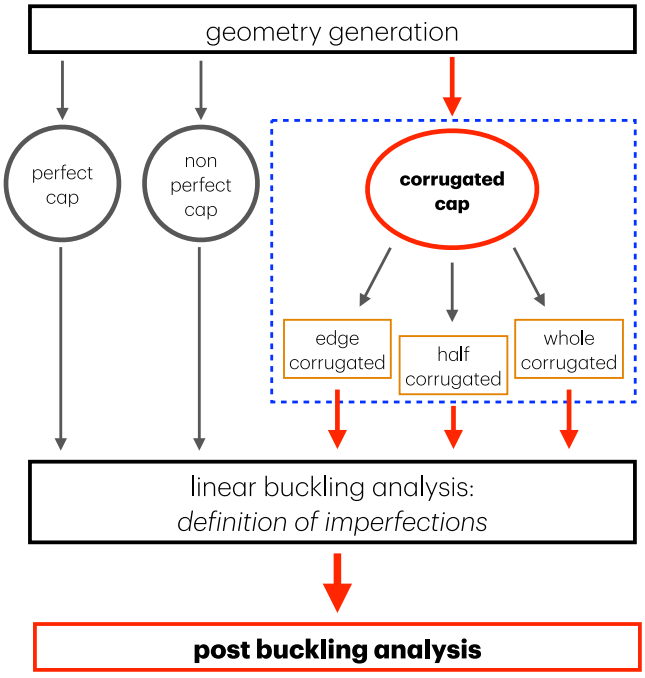

Fig. 4. Analysis procedure.

2. Parametric stability evaluation of corrugated-edge shells

2.1. Geometrical description

The geometric description of a shallow shell with assigned span is described here, and will be used as a model for the subsequent numerical examples. The structure is constructed to resemble the Flaminio dome, keeping constant the span, roughly equal to 60 m and varying the rise, in such way that a set of cases with variable rise-to-span ratio can be described.

Considering now a shell cross-section that lies within the xz plane. Let l and f be respectively the half-span and the rise of the dome ($l < R$), and let $x_0 = 0, z_0 = 0$ be the centre of a circle, therefore the circle equation is given by:

$$x^2 + (z - z_0^2) = R^2 \tag{3}$$

consequently, for a circle whose centre is located in the negative part of the z axis, the half-span-to-rise ratio is expressed functionally by f and R in the following way:

$$\frac{l}{f} = \frac{+\sqrt{R^2 - (f - R)^2}}{f} = \frac{+\sqrt{-f^2 + 2fR}}{f} = \sqrt{\frac{2R}{f} - 1}. \tag{4}$$

The formula gives real values for $0 < f \leq 2R$, and it is possible now to express the circle radius depending on the half-span and on the rise:

$$R = \frac{l^2 + f^2}{2f}. \tag{5}$$

Therefore, different ratios with an assigned half-span can be attributed, and the corresponding radius can be derived. Table 1 shows the values of four different geometries starting from a complete semi-circle, A, to a circle, D, whose rise is 5 m, all of them having a half-span of 30 m. The four cases A, B, C, and D, are depicted in Fig. 2. The obtained values could be replaced in the parametric equations reported in [27–29] and by using the procedure therein referred to, a geometrical model of the surfaces can be produced to perform FE analyses. Since, the instability of spherical shells is sensitive to the rise-to-half-span ratio f/l, *i.e.* the

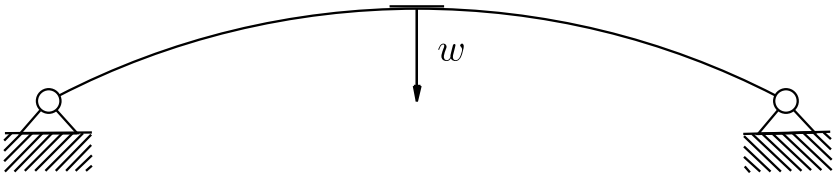

Fig. 5. Convention for the displacement orientation at the apex of the dome.

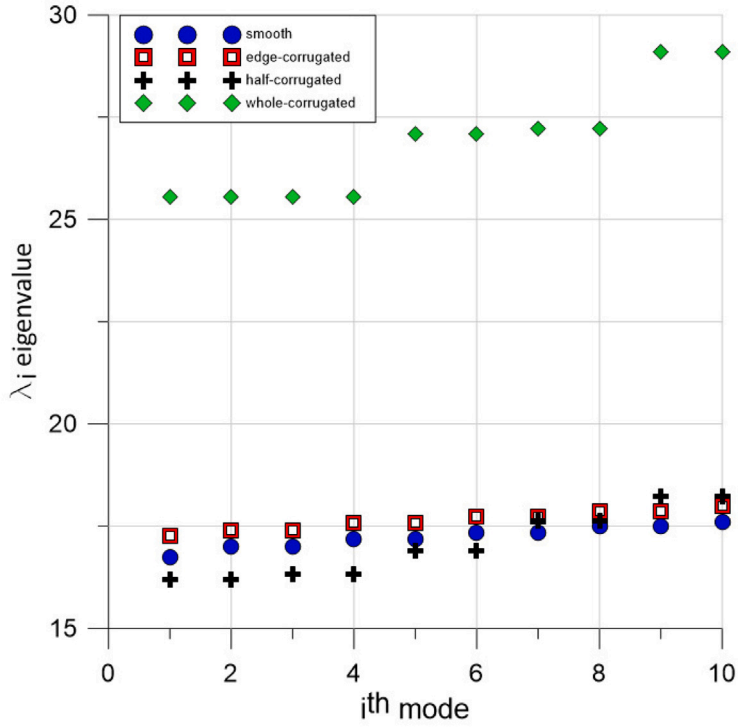

Fig. 6. The first ten eigenvalues derived from a linear buckling analysis for the four cases: smooth, edge-corrugated, half-corrugated and fully corrugated.

smaller the ratio, the more easily instability is triggered. Therefore, the last case, D, whose rise-to-half-span ratio f/l is equal to 0.17, is considered here. Moreover, the geometry of case D is comparable with the Nervi's Flaminio dome, that has a radius of 48.5 m, an half-span of 29.25 m, and a rise of 5.8 m, leading to a rise-to-half-span ratio f/l equal to 0.19.

In the following numerical analyses will be considered only for case D, that constitutes the most delicate case towards buckling phenomena. In order to figure out the effect of the corrugation on the dome non-linear behaviour, firstly the smooth case will be analysed, secondly corrugation will be introduced at the edge and then corrugation will be extended to half of the surface and finally, to the whole surface.

The parameter used to set the extension of the corrugation is the colatitude angle ϑ_0, see Fig. 3. The corrugated spherical shell cases are henceforth identified as: smooth, edge-corrugated, half-corrugated, and fully corrugated. Excluding the first case, the corrugation starting angle are respectively: ϑ_0, $\vartheta_0/2$ and 0.

2.2. Instability analysis: general framework

Instability investigations will be conducted as follows:

Table 4
First maximum load multiplier and first minimum load multiplier extracted from the equilibrium paths of a corrugated shell, to which an imperfection from the first to the fifth eigenshapes was individually applied.

		1st	2nd	3rd	4th	5th
λ_{max}	Smooth	4.38023	3.86702	6.36546	3.29877	3.29428
	Edge-corrugated	10.49390	5.21167	5.21167	6.22284	6.22284
λ_{min}	Smooth	1.64345	3.67448	3.34554	1.61897	1.51548
	Edge-corrugated	4.01866	3.15565	3.15565	2.54318	2.71113

1. analysis of stability issues (including a search for bifurcations) for *perfect* spherical caps of different amplitude with different load patterns (external pressure acting on the whole cap or on a subset of it and dead-weight load);
2. analysis of stability issues for *imperfect* spherical caps, with emphasis on sensitivity on location and amplitude of imperfection (for instance: displacement imposed to the edge, dimple-like imperfection, a hole in the shells), even for random imperfections;
3. analysis of stability issues for *perfect* edge-corrugated spherical caps, with a sensitivity evaluation based on the depth, angular extension, and number of waves.

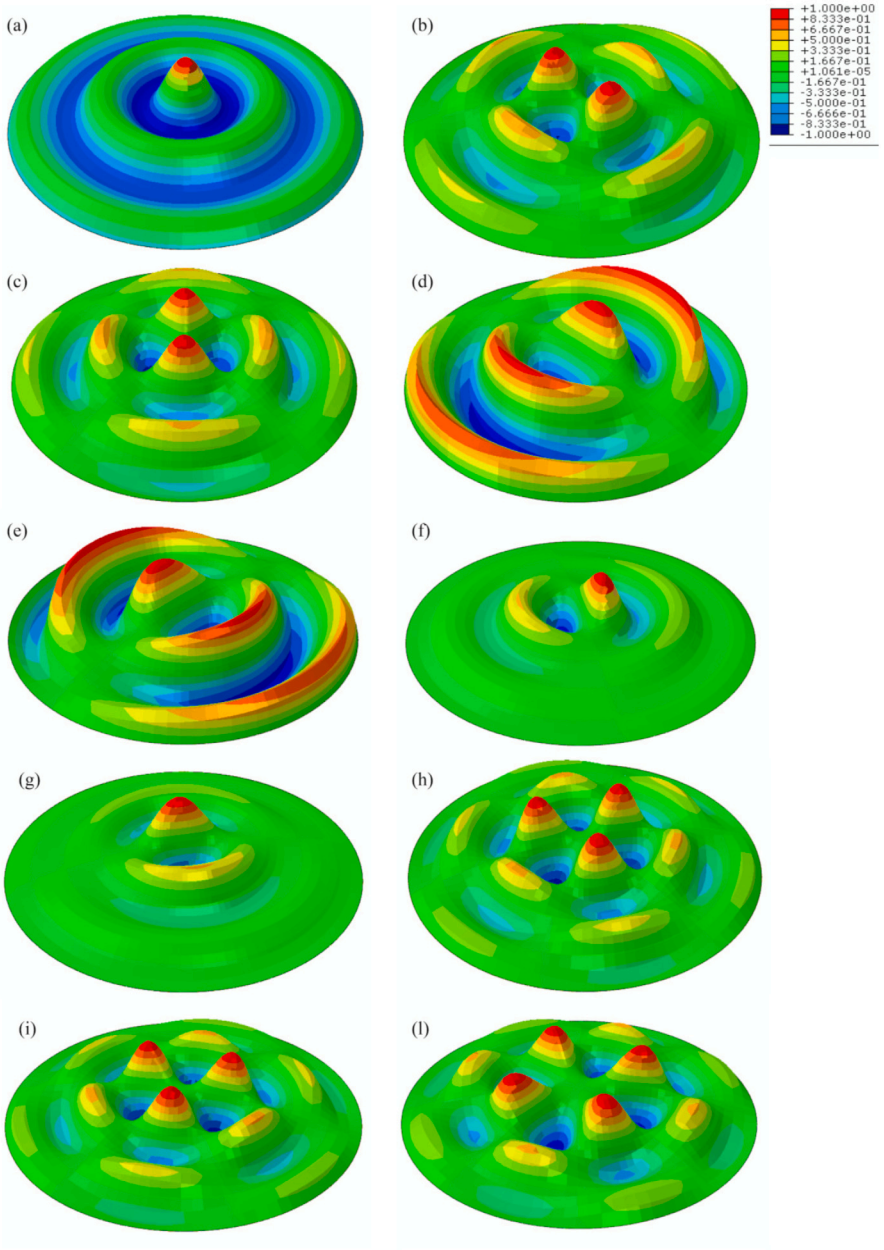

Fig. 7. Eigenshapes of a smooth shell, 1st (a), 2nd (b), 3rd (c), 4th (d), 5th (e), 6th (f), 7th (g), 8th (h), 9th (i) and 10th (l). The contour plot shows the magnitude of the displacement in z direction.

Table 5
First maximum load multiplier and first minimum load multiplier extracted from the equilibrium paths of a corrugated shell, to which an imperfection from the sixth to the tenth eigenshapes was individually applied.

		6th	7th	8th	9th	10th
λ_{max}	Smooth	4.01016	3.84184	4.34948	4.62767	4.96369
	Edge-corrugated	5.99063	5.99063	5.69488	5.69499	5.52714
λ_{min}	Smooth	3.44032	3.08219	4.53428	4.44666	3.43911
	Edge-corrugated	2.68605	2.68605	3.58923	3.34211	4.55273

The procedure to perform an analysis with imperfection in Abaqus is:

1. define an imperfection based on eigenmode shapes: when the imperfections are not known in advance, then it is possible to use, as an imperfection, the first eigenshape (which is given by a linear buckling analysis) or a combination of weighted eigenshapes;
2. defining an imperfection based on static analysis data. It consists in assigning a prescribed displacement to the whole set of nodes or to a chosen subset (for instance: only on the edge, or only upon a parallel, etc.), the displacement field computed by a static analysis;
3. define an imperfection directly: when the kind of imperfection is already known, that should be given to the model. It can be expressed as a displacement field in a chosen reference system; All

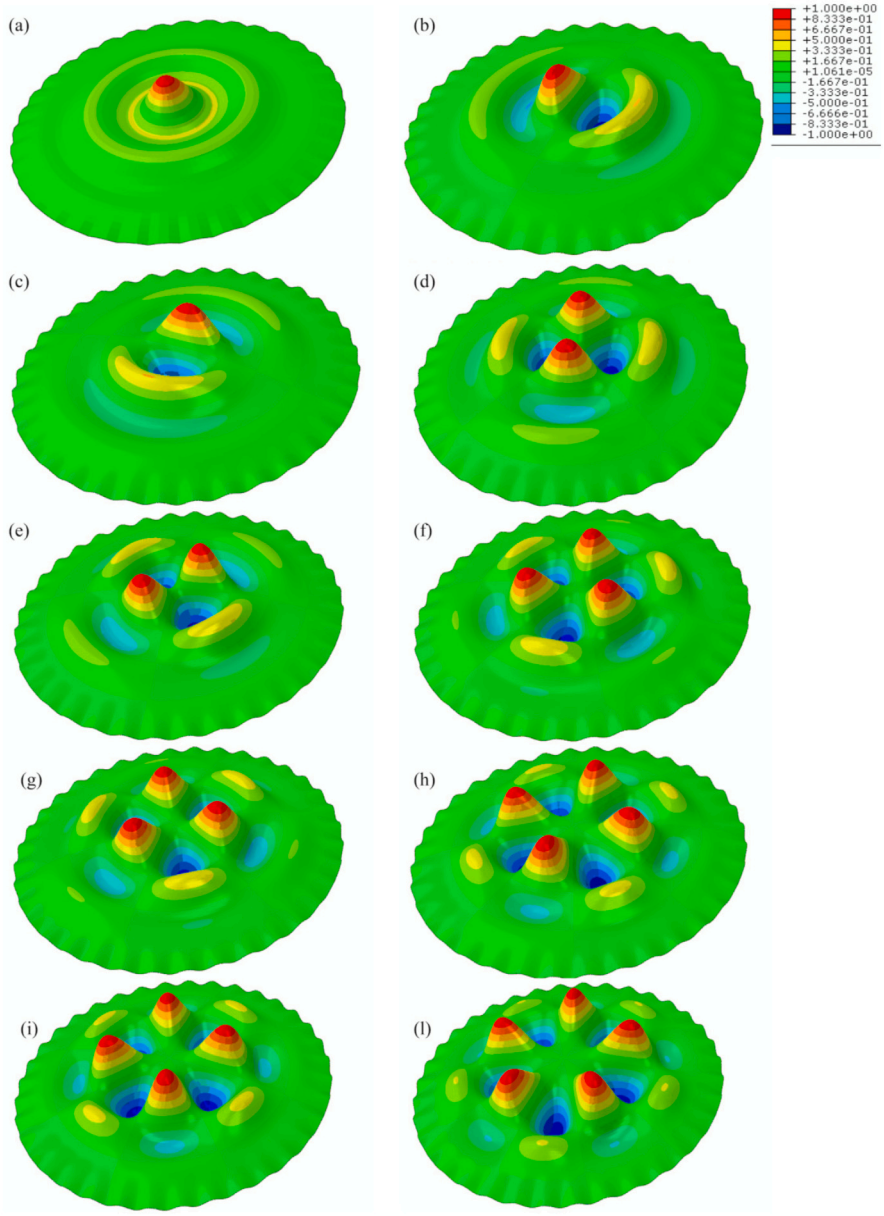

Fig. 8. Eigenshapes of an edge-corrugated shell, 1st (a), 2nd (b), 3rd (c), 4th (d), 5th (e), 6th (f), 7th (g), 8th (h), 9th (i) and 10th (l). The contour plot shows the magnitude of the displacement in z direction.

the previously mentioned models can be implemented working only on the "input" file of the model;

4. use customised perturbations.

The procedure and methodology adopted in henceforth has been in accordance with [17,30,31]. The above described procedure is summarised in the flowchart provided in Fig. 4.

In order to address properly the problem, it is necessary to recall some recent approaches that are currently used in non-linear analyses of shell structures. The studies presented in the scientific literature are mainly devoted to understanding the effect of imperfection in pre-critical behaviour on spherical shells, here some references have been selected.

In the following analysis, the non-linear material behaviour of concrete will not be addressed. In fact, the research campaign on the plastic behaviour of Nervi's structures is lacking, and there are no available data on real specimens or real structures. Nonetheless, the aim is to figure out the effect of instability on spherical shells of the wavy shape. In contrast, it is well-clear to the authors that plasticity affects the actual behaviour of such structures, though for the purpose of this research, it is sufficient to decouple the non-linearities considering only the geometrical one.

The equilibrium curves (*i.e.* a plot of the structure equilibrium position depending on the load multiplier and evolutive parameters) are limited only to displacements not greater than 1 m. Considering thin concrete shells, this assumption does not seem reasonable, but to fully understand the post-critical behaviour, it is worth extending the displacement range beyond the admissible displacement for reinforced concrete. Otherwise it is not possible to correctly characterise the phenomenon.

For instance, sudden instability, such as the snap-through, is characterised by an everted portion of the shell (*i.e.* a signum change of

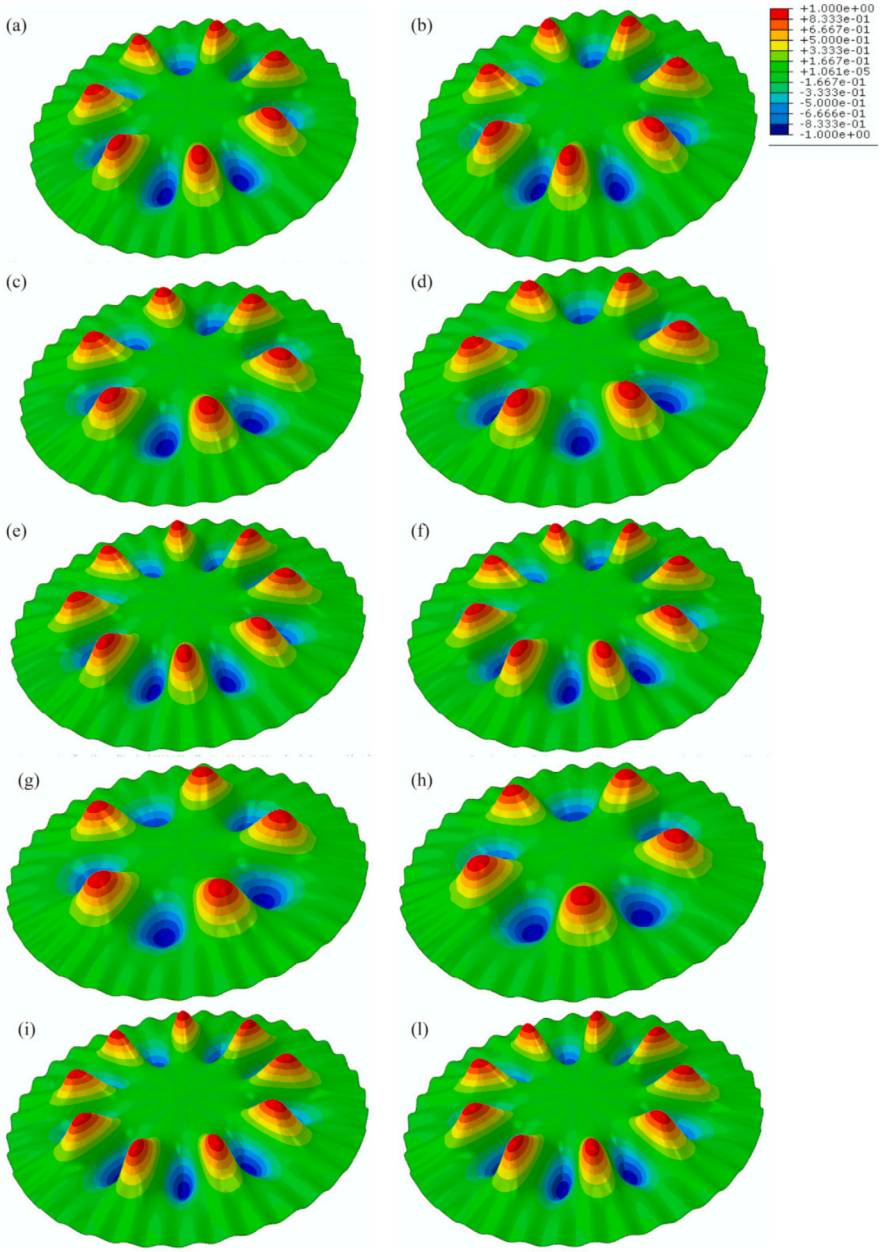

Fig. 9. Eigenshapes of a half-corrugated shell, 1st (a), 2nd (b), 3rd (c), 4th (d), 5th (e), 6th (f), 7th (g), 8th (h), 9th (i) and 10th (l). The contour plot shows the magnitude of the displacement in z direction.

the surface curvature). Even though it is an issue that has still to be addressed in the design process, it is likely, and to accurately assess its chance to occur, that the analysis must consider large displacements (a hypothesis not usually adopted in the RC design) and the complete shape of the equilibrium curve. Furthermore, once the structure has become unstable, mechanical reserves of strength still exist after the buckling load has been reached. The choice of the evolutive parameter for the equilibrium curves requires some clarifications. In fact, in the case of a simple structure such as a frame or an articulated beam, it is relatively easy to select the parameters due to the limited number of nodes to choose from, or the easiness to compute other significant quantities, namely strain, volume etc. For example, if a truss girder is loaded with a concentrated load, the parameter should be the displacement in the load direction. See the well-known case of a von Mises truss and Lee's frame.

However, this is different when shells are dealt with; theoretically, a shell is a continuous structure with various modes of buckling which differ significantly from one another. Each buckling mode requires a separate parameter, limiting the possibility of comparing the various graphs. For example, in the case of a localised snap instability, the choice falls on the point of maximum displacement around the snapped area. In the following discussion about the dome instability behaviour, considering that the option is not unique, the sensitivity and the insight of the designer has to guide the suitable choice. Henceforth, the displacement of the dome vertex is chosen as the monitored point, see Fig. 5. This is the point generally subjected to the most significant displacement, but the reader should keep in mind that the choice is not unique.

Even though the equilibrium curves are pushed beyond the admissible displacement for concrete it must be clear that failure mode will

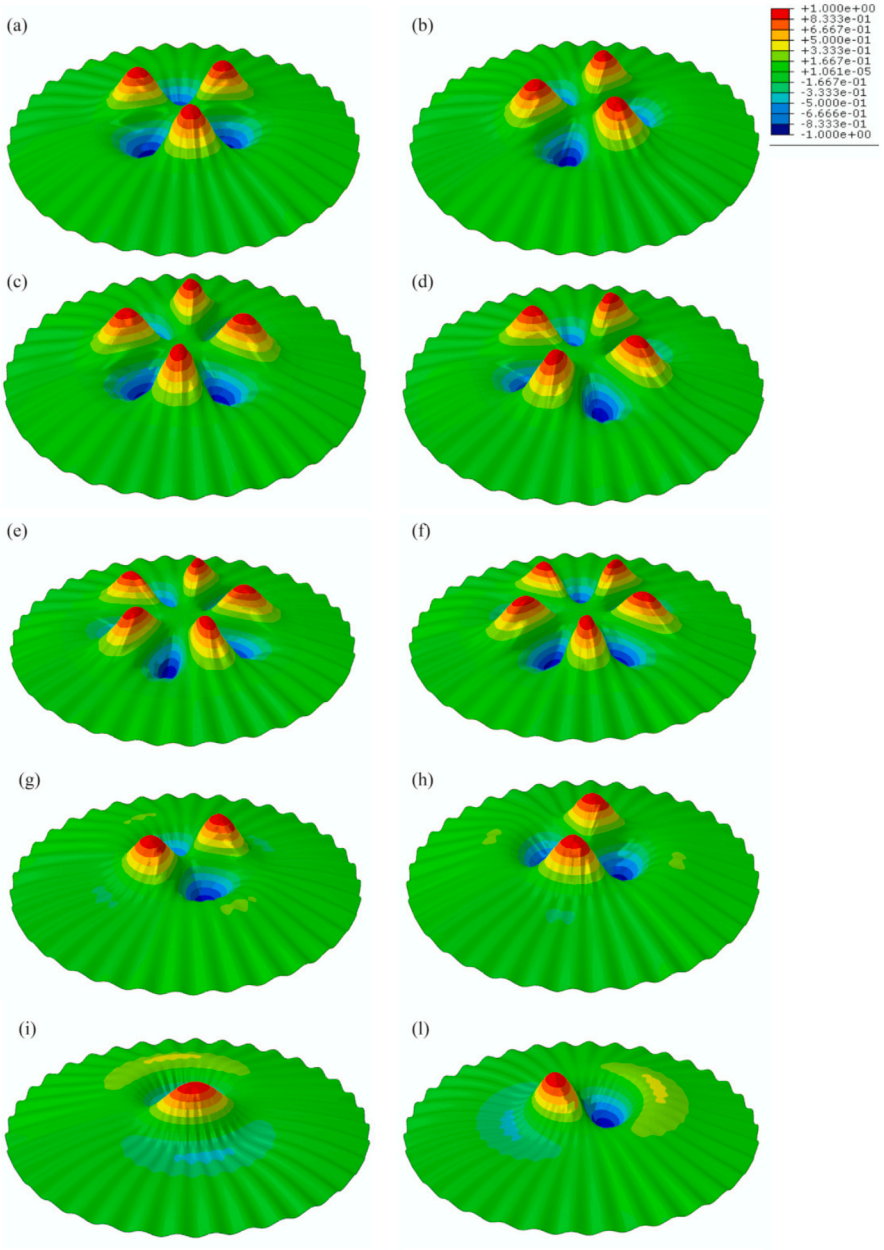

Fig. 10. Eigenshapes of a fully corrugated shell, 1st (a), 2nd (b), 3rd (c), 4th (d), 5th (e), 6th (f), 7th (g), 8th (h), 9th (i) and 10th (l). The contour plot shows the magnitude of the displacement in z direction.

not be due to instability but, most likely, to overcoming the strength of concrete. The failure may be produced by forming a plastic hinge or by fragility, especially in the area where the stress is localised (*i.e.* supports). At preliminary step, we provided convergence analysis considering various numbers of elements and their type, as done in [28,29]. The further analysis was provided for a given number of elements and the same type of finite elements. The FE model number of elements is similar for corrugated shells and for smooth ones, so a choice of 94 elements for each hoop circle and 30 in the meridian direction has been adopted. A 4-node shell element based on [32,33] is used. Notice that the 8-node shell element, which better represents the shape in case of a surface with double curvature due to the its second order shape functions, is not employed.

Investigations to consider the impact of geometrical non-linearities, limiting only to geometrical imperfections, are addressed. The following cases can be distinguished: (1) linear buckling analysis of perfect shells (shorten to *buckling analysis*), (2) linear analysis with geometrical imperfections, (3) geometrically non-linear analysis, (4) geometrically non-linear analysis with imperfections.

2.3. Linear instability analysis

Table 2 shows the results of a linear buckling analysis for two different boundary conditions, namely, hinged and clamped edge; it reports the load multipliers (eigenvalues) for which the model stiffness matrix becomes singular. The hydrostatic pressure load case is considered.

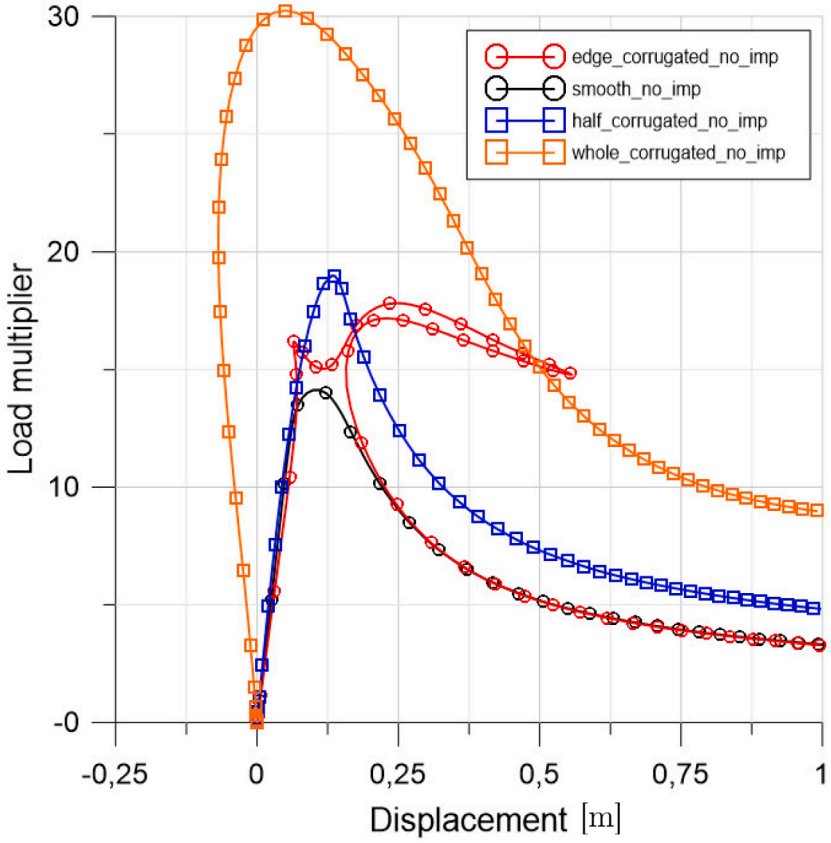

Fig. 11. Equilibrium paths of perfect shells: smooth (black solid line), an edge corrugated (red solid line), a half corrugated (blue solid line) and a wholly corrugated (orange solid line). (For interpretation of the references to colour in this figure legend, the reader is referred to the web version of this article.)

The theoretical values can be obtained considering the fully restrained conditions; nonetheless, even for the hinged shells, the values do not significantly differ. In the design practice, the actual support conditions are not easily classified, see, for instance, some references about the historical techniques of construction for concrete supports [34] and should be analysed experimentally. The worst condition is that of hinged supports; therefore, the subsequent analyses will consider only this case.

Table 3 presents the eigenvalues for the first ten modes for each of the considered shapes under self-weight loading. The corrugation gradually vary from a smooth one to a fully corrugated surface, through the intermediate cases: the edge-corrugated shape that resembles the Nervi's Flaminio dome and the half-corrugated dome. It should be noticed that all the values are close to each others, and after the first value, the eigenvalues show a double multiplicity; this evidence is known to be associated to a high sensitivity to imperfections.

Fig. 6 demonstrates graphically the obtained numerical results; it is evident that the critical load value increases as the corrugation spreads across the surface. This increase is remarkable in the case of the fully-corrugated shells, about 50% with respect to the smooth one.

Figs. 7 and 8 provide the buckling eigenshapes for the first 10th modes of the smooth and the edge-corrugated dome. The contour plot displays the displacement field in the vertical direction. The first eigenshape is always symmetrical [14]. The edge-corrugated shell is also the case, with the difference that the displacements are smaller near the edge. Consequently, the wavy shape restricts the buckled surface to a minor area. Figs. 9 and 10 show the analogous eigenshapes for the half and wholly corrugated dome. In the third case, the new shape locks all the buckled shapes that involve the wavy area; this forces the structure to buckle with higher modes (concerning the smooth case modes). This effect is amplified for the fully corrugated domes, where much higher modes involve only the area surrounding the apex. Besides, these modes are not likely to be triggered.

2.4. Equilibrium paths

In Fig. 11 we present four equilibrium paths, i.e. load–displacement curves, for corrugated shells without imperfections. One can see that corrugation dramatically changes the mechanical response. Note that hereinafter displacements are taking in the apex as in Fig. 5 and given in metres, whereas the load multiplier is dimensionless.

Instead in the next figures we show equilibrium paths for shells with imperfections. Figs. 12, 13, and 14 show the applied load as a function of the displacement for different cases. The applied imperfection is based on the nth buckling mode of the linear analysis, to which a scale factor has been applied that reduces the buckling modes to obtain the desired imperfection size. This value has been set to 0.1, so the imperfection consists of a displacement field applied to the initial configuration. Figs. 15, 16, and 17 show the same equilibrium path considering only one parameter of the mechanical system (which is always increasing) instead of the displacement of a control point, in this case the measure *arc length*, although not having an immediate mechanical meaning, constitutes a continuous and evolving parameter that can make the output of the equilibrium path more readable.

Tables 4 and 5 show the first two load values of the limit points for each equilibrium path (*i.e.* the first is the first maximum value and the second one is the minimum one).

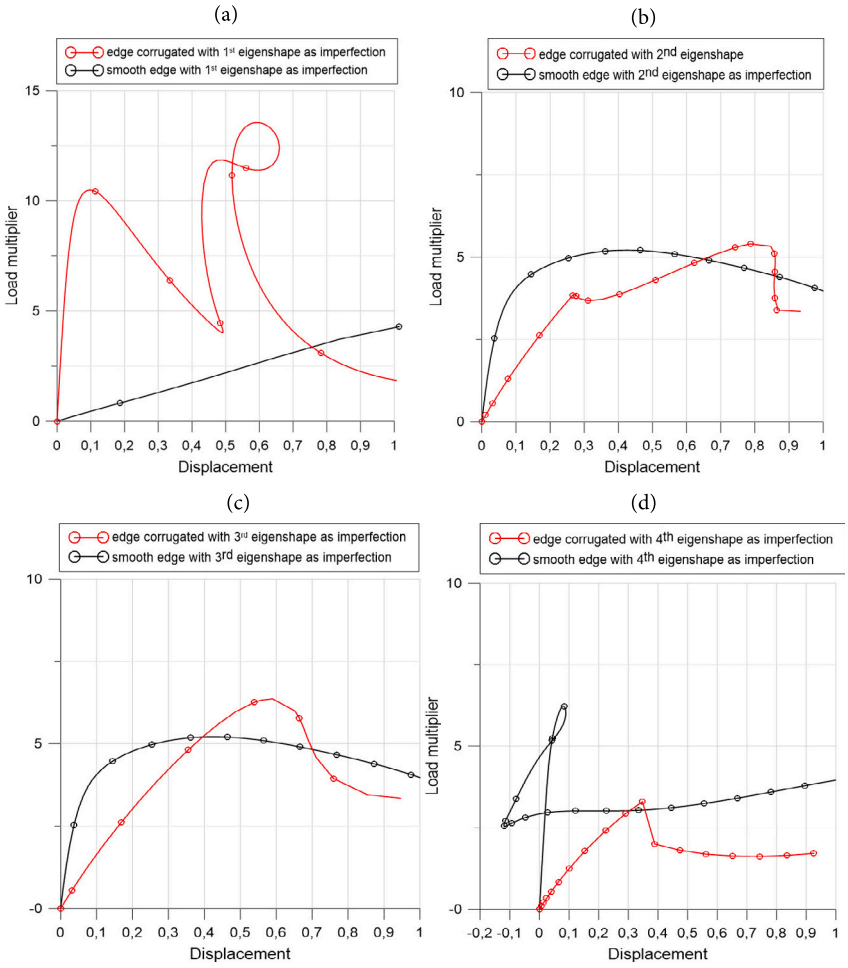

Fig. 12. Equilibrium paths of a smooth shell (black solid line) and of an edge corrugated shell (red solid line). The following imperfections have been individually applied: 1st (a), 2nd (b), 3rd (c) and 4th (d) eigenshapes. (For interpretation of the references to colour in this figure legend, the reader is referred to the web version of this article.)

If we restrict ourselves to considering vertex displacements to the range in $30 \div 40$ cm (corresponding to an approximate maximum admissible displacement equal to $1/200$ of the dome span), it appears that, for the smooth dome, the most critical case is that shown in graph (a). For the corrugated dome, case (d) appears to be the most severe.

One could therefore observe that for the smooth dome, the most detrimental imperfections are those that approximate the first mode, while for the corrugated dome, on the other hand, are those that have a shape close to the fourth mode.

Comparing the two equilibrium curves, then, one sees that the corrugated dome has a critical load of about twice that of the smooth dome. The behaviour significantly changes when the corrugation is applied to the whole surface and not only to a minor part of the shell, *i.e.* the edge. The previous considerations about post-buckling behaviour show that the corrugation on a portion of the shell leads to an improvement of about $2 \div 4\%$, that is not significant in practical applications. On the contrary when the whole corrugation is analysed the load corresponding to the limit and the bifurcation point shows greater values.

The post-buckling curves of the mechanical response considering each time the first five eigenshapes are depicted in Fig. 18. What is striking in these curves is the greater values of the load at which the instability occurs; indeed, regarding the first imperfection, the value is three times the respective one for the smooth shells; the same happens when the second and fifth eigenshapes are used. Whereas, with the third eigenshapes, the value is more than two times. The more remarkable improvement is reached when the fourth imperfection is introduced; the buckling occurs at a value that is roughly five times the one obtained when no corrugation is adopted.

3. Conclusions

Using parameterisation of corrugated shells proposed recently in [27,28,35], which accurately handles the doubly curved geometry, we presented a suitable FE simulation procedure for buckling and post-buckling analysis of shallow shells. As a result, we provide the detailed analysis of buckling of shallow spherical shells considering three types of corrugations. In addition considering an eigenshape as initial imperfection we discussed the sensitivity to imperfections. It has been shown through numerical simulation what was probably intuitively clear to P. L. Nervi: a corrugation along the edge improves the structural performance of a shell. As a result, corrugated shell structures can be both used as a canopy also endowed with some aesthetics and can be introduced in buildings for their high-performance mechanical properties, like in the case of roofs for special and spatial structures.

Considering further applications of our results it is worth to mention the automatisation of building processes. Indeed, the presented above procedure may be applied to perform more extensive parametric

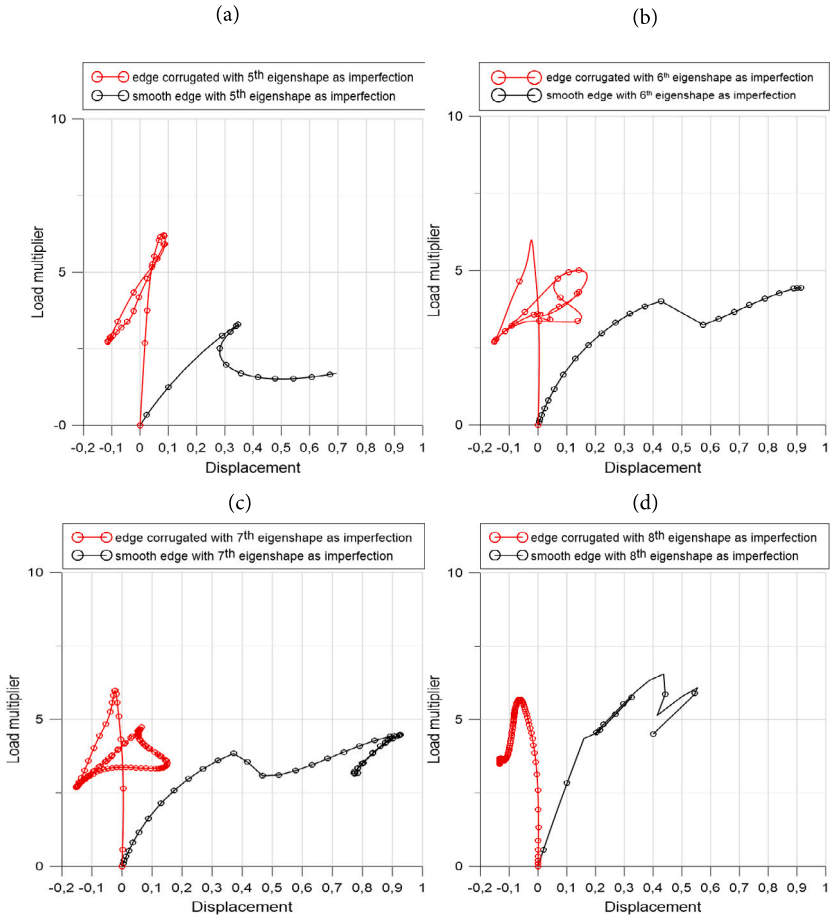

Fig. 13. Equilibrium paths of a smooth shell (black solid line) and of an edge corrugated shell (red solid line). The following imperfections have been individually applied: 5th (a), 6th (b), 7th (c) and 8th (d) eigenshapes. (For interpretation of the references to colour in this figure legend, the reader is referred to the web version of this article.)

analysis of different corrugation geometries that may lead to even more complex behaviours, as well to analyse different shapes, such as free-form shells [36,37] and concrete printed structures. Some improvements could be achieved in the LIDAR (Laser Imaging Detection And Ranging) field to accurately identify the influence of small deviations in the structural behaviour; a comparison between a theoretical shape and *in situ* surveys could be done [38]. A main issue related to the topic discussed in the present work involves the role of corrugation in instability phenomena, and it was intended to highlight the statical intuition envisioned by P.L. Nervi. The effect of edge-corrugation is assessed only through linear elastic stress analysis. Besides, buckling has been explicitly addressed, and for this purpose, imperfections have been considered to trigger the instability phenomena. The corrugation effect has been highlighted without imperfections and with a customised set of imperfections, showing a relevant effect in switching the eigenshapes to higher modes, reducing the displacements and increasing the ultimate load. Indeed, it constitutes a very challenging problem whose solution has yet to be achieved.

The methods developed in this paper for civil engineering and architecture applications can be relatively simply generalised to be used in different scientific milieux. Moreover, the presented study may be extended towards advanced theories of shells. Given the relevance of this problem in thin-shell structures [39], the buckling behaviour could be studied more comprehensively in forthcoming research to ascertain how the discussed geometry affects the stability of such shells and to discuss a prospective corrugation optimisation.

CRediT authorship contribution statement

Matteo Lai: Formal analysis, Investigation, Methodology, Software, Writing – original draft. **Nicola Luigi Rizzi:** Supervision, Validation. **Victor A. Eremeyev:** Supervision, Validation, Writing – original draft, Writing – review & editing, Funding acquisition, Conceptualization. **Emanuele Reccia:** Data curation, Supervision, Validation, Writing – original draft, Writing – review & editing. **Antonio Cazzani:** Formal analysis, Supervision, Validation, Conceptualization.

Declaration of competing interest

The authors declare that they have no known competing financial interests or personal relationships that could have appeared to influence the work reported in this paper.

Acknowledgements

V.A.E., E.R., and A.M.C. acknowledge the financial support under the National Recovery and Resilience Plan (NRRP), Mission 4, Component 2, Investment 1.1, Call for tender No. 1409 published on 14.9.2022 by the Italian Ministry of University and Research (MUR), funded by the European Union – NextGenerationEU – Project Title "A Fluid-Structure Interaction tool for the protection of Clean Energy Production sites (FSI-CEP)" – CUP F53D23009640001- Grant Assignment Decree No. P20227CSJ5 adopted on 14 September 2022 by the Italian Ministry of University and Research (MUR).

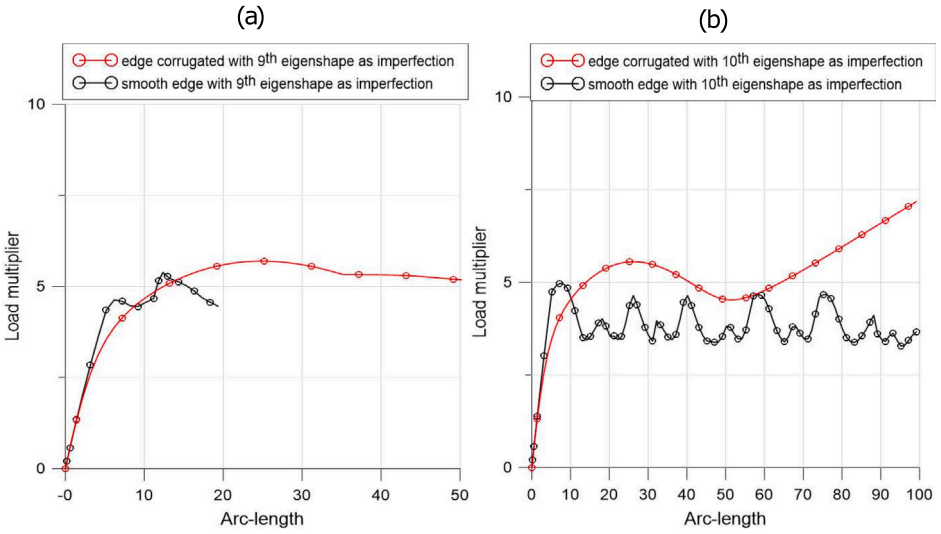

Fig. 14. Equilibrium paths of a smooth shell (black solid line) and of an edge corrugated shell (red solid line). The following imperfections have been individually applied:x 9th (a) and 10th (b) eigenshapes. (For interpretation of the references to colour in this figure legend, the reader is referred to the web version of this article.)

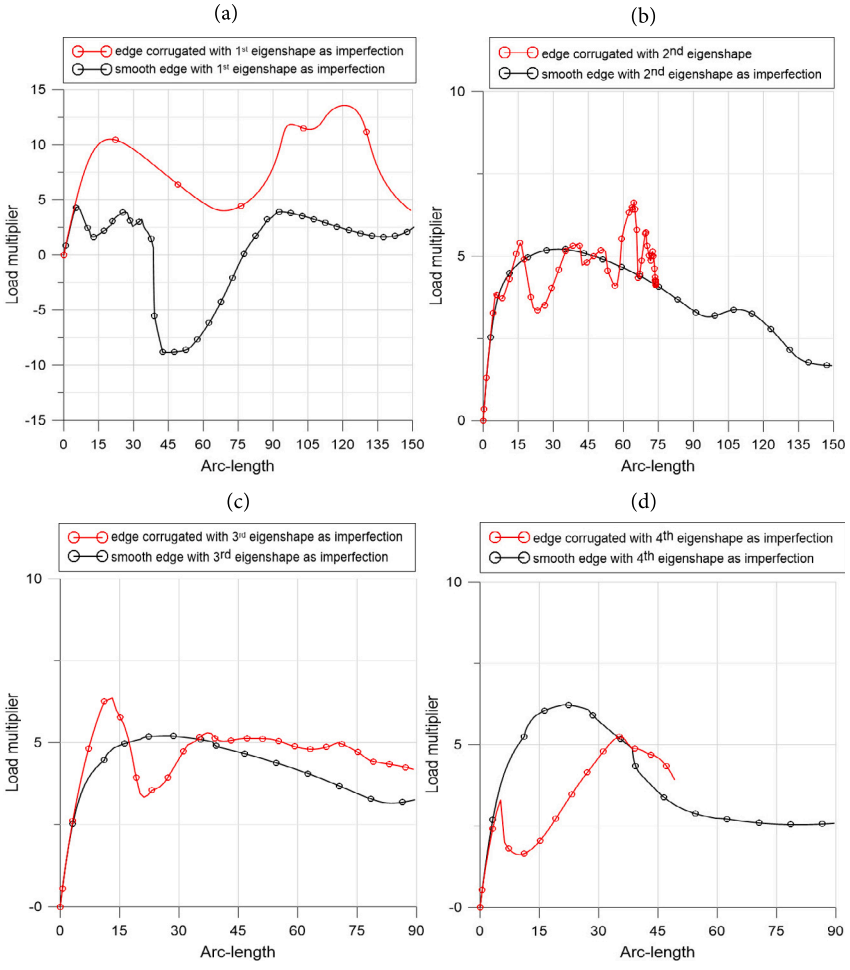

Fig. 15. Equilibrium paths of a smooth shell (black solid line) and a edge corrugated shell (red solid line), using the arc-length. The following imperfections the 1st (a), 2nd (b), 3rd (c) and 4th (d) eigenshapes was individually applied. (For interpretation of the references to colour in this figure legend, the reader is referred to the web version of this article.)

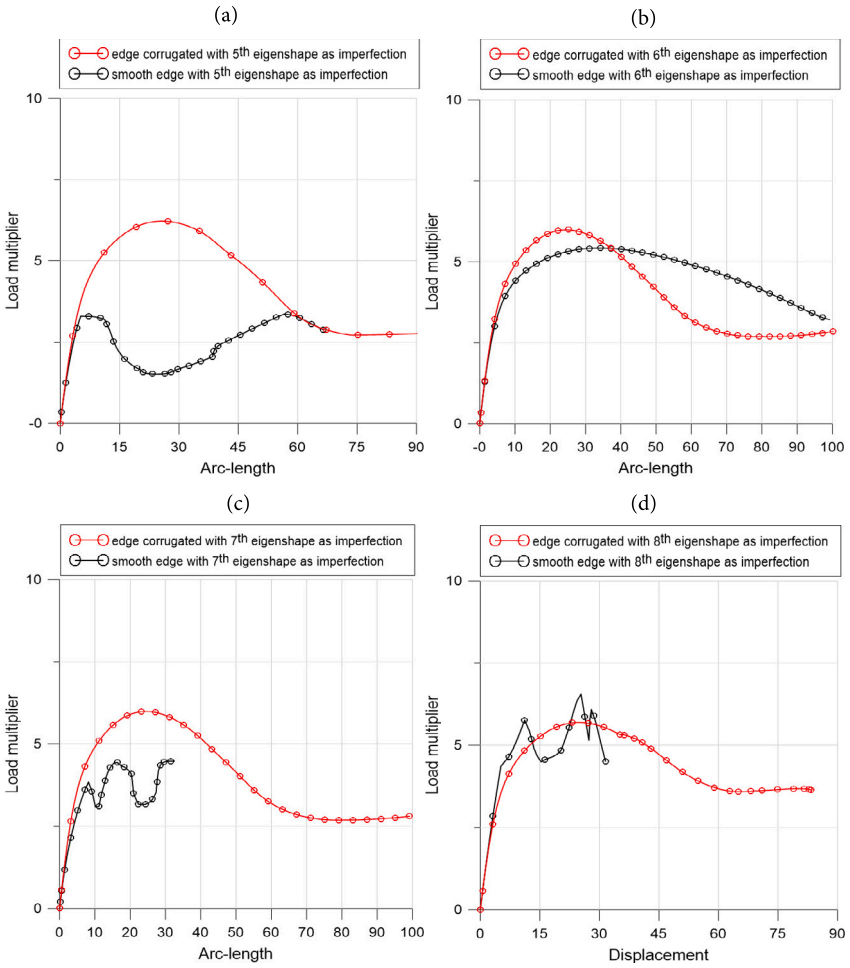

Fig. 16. Equilibrium paths of a smooth shell (black solid line) and a edge corrugated shell (red solid line), using the arc-length. The 5th (a), 6th (b), 7th (c) and 8th (d) eigenshapes was applied as imperfections. (For interpretation of the references to colour in this figure legend, the reader is referred to the web version of this article.)

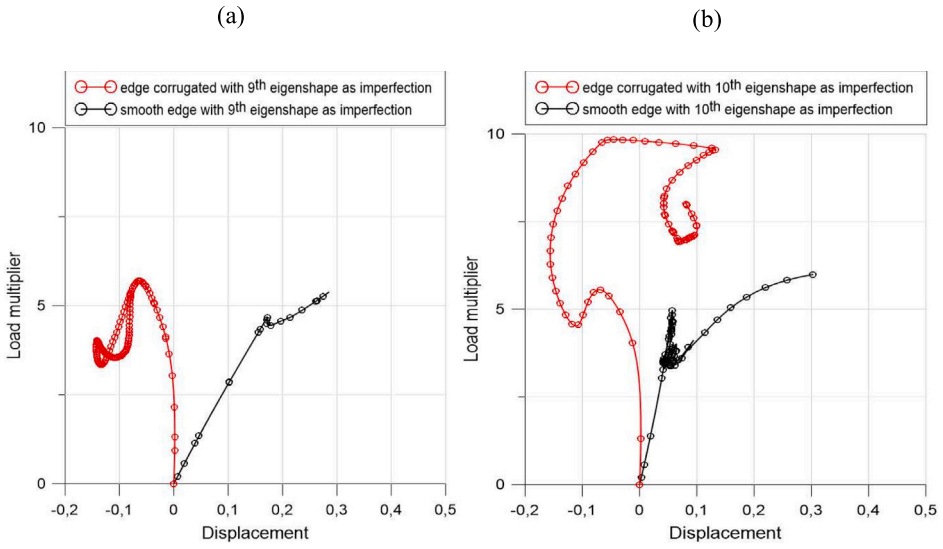

Fig. 17. Equilibrium paths of a smooth shell (black solid line) and a edge corrugated shell (red solid line), using the arc-length method. As imperfections the 9th (a) and 10th (b) eigenshapes was applied. (For interpretation of the references to colour in this figure legend, the reader is referred to the web version of this article.)

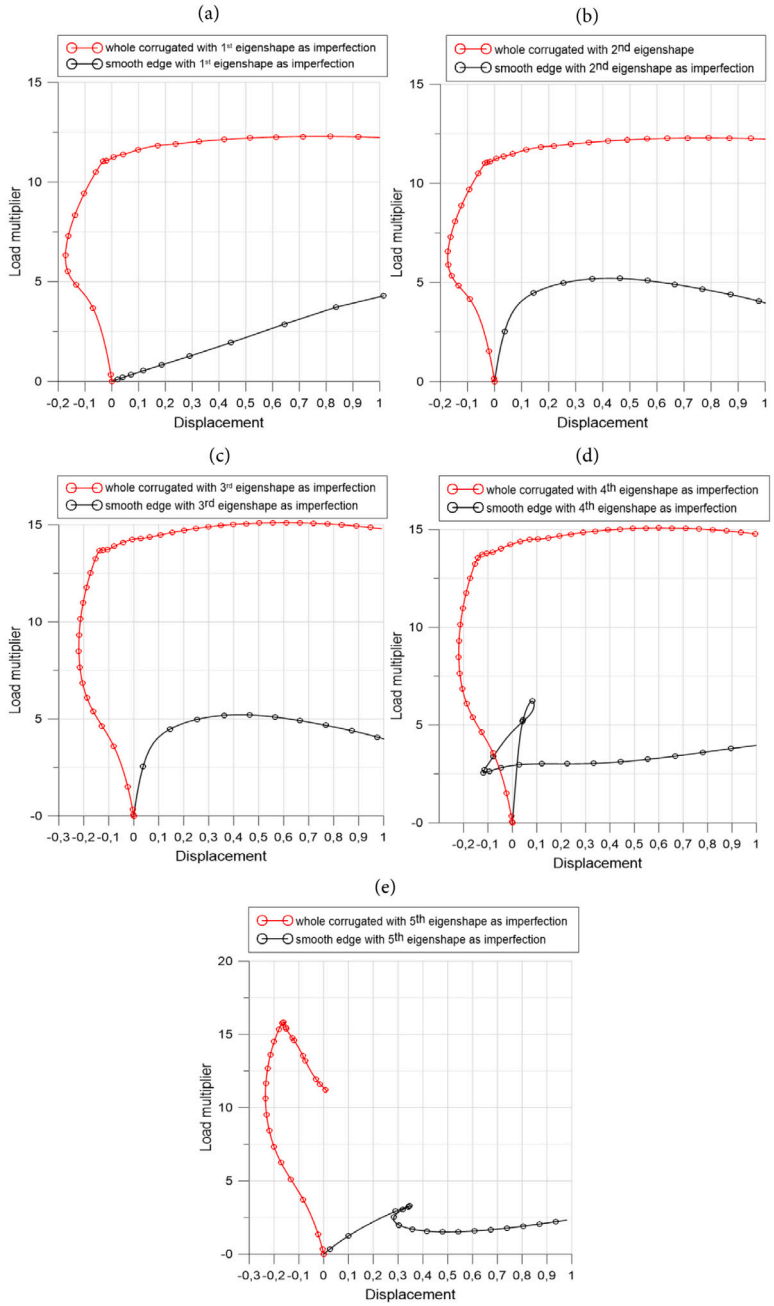

Fig. 18. Equilibrium paths of a smooth shell (black solid line) and a wholly corrugated shell (red solid line). The 1st (a), 2nd (b), 3rd, 4th, 5th eigenshapes was applied as the imperfections. (For interpretation of the references to colour in this figure legend, the reader is referred to the web version of this article.)

References

[1] Timoshenko SP, Gere JM. Theory of elastic stability. 2nd ed.. Aucklend: McGraw-Hill; 1963.

[2] Bažant ZP, Cedolin L. Stability of structures. elastic, lnelastic, fracture and damage theories. World Scientific Publishing; 2010.

[3] Samuelson LA, Eggwertz S, editors. Shell stability handbook. London: Elsevier Applied Science; 1992.

[4] Amabili M. Nonlinear vibrations and stability of shells and plates. Cambridge: Cambridge University Press; 2008.

[5] Koiter WT. On the nonlinear theory of thin elastic shells. Proc K Ned Akad Wet B 1966;69:1–54.

[6] Koiter WT, Simmonds JG. Foundations of shell theory. In: Becker E, Mikhailov GV, editors. Theoretical and applied mechanics. Berlin: Springer; 1973, p. 150–76.

[7] Koiter WT, van der Heijden AMA. W. T. Koiter's elastic stability of solids and structures. Cambdridge: Cambridge University Press; 2009.

[8] Zoelly R. Uber ein knickproblem an der kugelschale (Ph.D. thesis), Technischen Hochschule in Zürich; 1915.

[9] Schwerin E. Zur stabilität der dünnwandigen hohlkugel unter gleichmäßigem außendruck. ZAMM - Z Angew Math Mech 1922;2(2):81–91.

[10] Van der Neut A. De elastische stabiliteit van den dunwandigen bol (Ph.D. thesis), TU Delft; 1932.

[11] Hutchinson JW. Imperfection sensitivity of externally pressurized spherical shells. J Appl Mech 1967;34(1):49–55.

[12] Sanders JL. Nonlinear theories for thin shells. Quart Appl Math 1963;21:21–36.

[13] Budiansky B. Notes on nonlinear shell theory. J Appl Mech 1968;35(2):393–401.

[14] Hutchinson JW. Buckling of spherical shells revisited. Proc R Soc A: Math Phys Eng Sci 2016;472(2195):20160577.

[15] Budiansky B. Buckling of clamped shallow spherical shells. In: The theory of thin elastc shells. 1960, p. 64–94.

[16] Reissner E. Symmetric bending of shallow shells of revolution. J Math Mech 1958;7(2):121–40.

[17] Wagner H, Hühne C, Niemann S. Robust knockdown factors for the design of spherical shells under external pressure: Development and validation. Int J Mech Sci 2018;141:58–77.

[18] Chróścielewski J, Eremeyev VA. Can we really solve an arch stability problem? Internat J Engrg Sci 2024;194:103968.
[19] von Kàrmàn T, Tsien H-S. The Buckling of spherical shells by external pressure. J Aeronaut Sci 1939;7:43–50.
[20] Tsien H-S. A theory for the buckling of thin shells. J Aeronaut Sci 1942;9(10):373–84.
[21] Koiter WT. On the stability of elastic equilibrium (Ph.D. thesis), Washington: Technishe Hooge School at Delft; 1967.
[22] Gioncu V. Thin reinforced concrete shells: special analysis problems. Bucarest: Wiley; 1979.
[23] Sawires MI. Traglastberechnung dünnwandiger ausgesteifter kugelschalen (Ph.D. thesis), Universität Karlsruhe; 1968.
[24] Ramm E. Ultimate load and stability analysis of reinforced concrete shells. In: Proc. IABSE colloquium on computational mechanics of concrete structures. 1987, p. 144–56.
[25] Heyman J. Equilibrium of shell structures. Oxford: Oxford University Press; 1977.
[26] Medwadowski SJ, editor. Recommendations for reinforced concrete shells and folded plates. Madrid: IASS; 1979.
[27] Lai M, Reccia E, Spagnuolo M, Cazzani A. Structural behaviour of corrugated shells: a look at the Flaminio dome in Rome. In: Proceedings of the 2nd fib Italy YMC symposium on concrete and concrete structures. 2021, p. 87–94.
[28] Lai M, Eugster SR, Reccia E, Spagnuolo M, Cazzani A. Corrugated shells: An algorithm for generating double-curvature geometric surfaces for structural analysis. Thin-Walled Struct 2022;173:109019.
[29] Lai M, Zucca M, Meloni D, Reccia E, Cazzani A. Thin corrugated-edge shells inspired by nervi's dome: Numerical insight about their mechanical behaviour. Thin-Walled Struct 2023;191:111076.
[30] Darmawan L, Tedianto LS. Critical buckling load analysis on spherical shells under various geometric imperfections. In: IOP conference series: materials science and engineering, vol. 1007, 2020, 012045.
[31] Qiao C, Liu L, Pasini D. Elastic thin shells with large axisymmetric imperfection: from bifurcation to snap-through buckling. J Mech Phys Solids 2020;141:103959.
[32] Belytschko T, Lin JI, Chen-Shyh T. Explicit algorithms for the nonlinear dynamics of shells. Comput Methods Appl Mech Engrg 1984;42(2):225–51.
[33] Belytschko T, Wong BL, Chiang H. Advances in one-point quadrature shell elements. Comput Methods Appl Mech Engrg 1992;96(1):93–107.
[34] Leonhardt F, Mönnig E. C.A. & C.A.P.: calcolo di progetto & tecniche costruttive. L'Armatura nelle costruzioni in cemento armato. Statica, tecnologia, tipologia. Vol. 3, Milano: Edizioni di scienza e tecnica; 1979.
[35] Lai M. Edge-corrugation as structural enhancement of shallow shells. Nexus Netw J 2023;25(1):455–61.
[36] Olivieri C, Angelillo M, Gesualdo A, Iannuzzo A, Fortunato A. Parametric design of purely compressed shells. Mech Mater 2021;155:103782.
[37] Olivieri C. Formerly-math: Constrained form-finding through membrane equilibrium analysis in mathematica. Softw Impacts 2023;16:100512.
[38] Lai M, Argiolas R, Musanti F, Meloni D, Reccia E, Cazzani AM. Corrugated shells: A reinforced concrete roof designed by Aldo Favini in Sesto S. Giovanni. In: Italian workshop on shell and spatial structures. 2023, p. 161–70.
[39] Rotter JM, Mackenzie G, Lee M. Spherical dome buckling with edge ring support. Structures 2016;8:264–74.